Planting MoS2 nanosheets towards standing vertically on substrate by a Dynamic Magnetic Field

*Ruifeng Qi[a], YongCheng[a], Jinhong Hou[a], Xiaohua Qiao[a], Junqi Liu[a]and QingsongHuang[*a,b]*

[a] School of Chemical Engineering, Sichuan University, Chengdu 610065, China.

[b] Tianfu Jiangxi Laboratory, Chengdu 610065, China

1. The MoS_2 nanosheets were grown on different substrate surfaces at reaction times of 60 seconds.

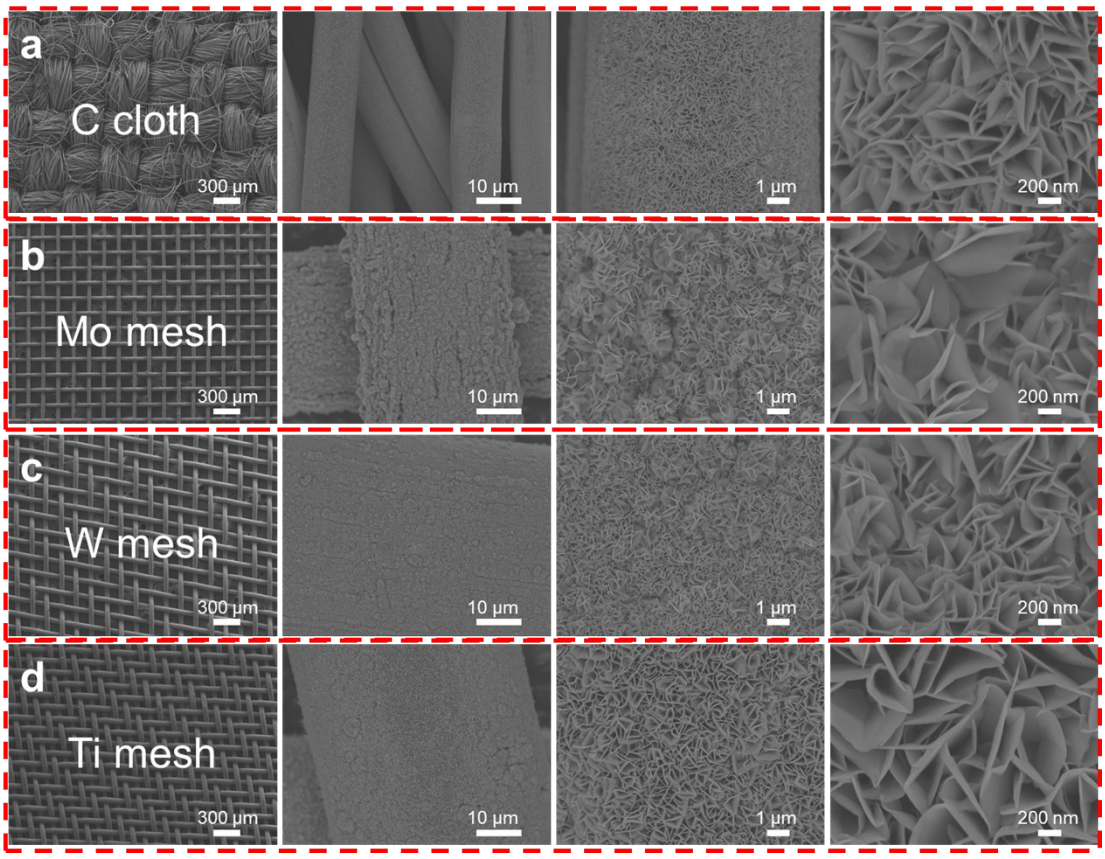

Fig. S1 shows the MoS_2 nanosheets grown on different substrate surfaces at reaction times of 60 seconds, including carbon fiber cloth, molybdenum mesh, wolfram mesh, and ferrous mesh, respectively.

2. Schematic representation of the interaction of a polar molecule of molybdenum trioxide with a dynamic magnetic field.

According to Maxwell's equations, MoO_3 molecules are polarized when placed in a dynamic magnetic field. When the excited magnetic field (H) increases gradually, an induction magnetic field (B) should be available to resist the H's increasing. Thus, the circle induction electric field should be available in the plane normalized to the H direction. The circle induction electric field can drive the MoO_3 molecule transportation under a dynamic magnetic field.

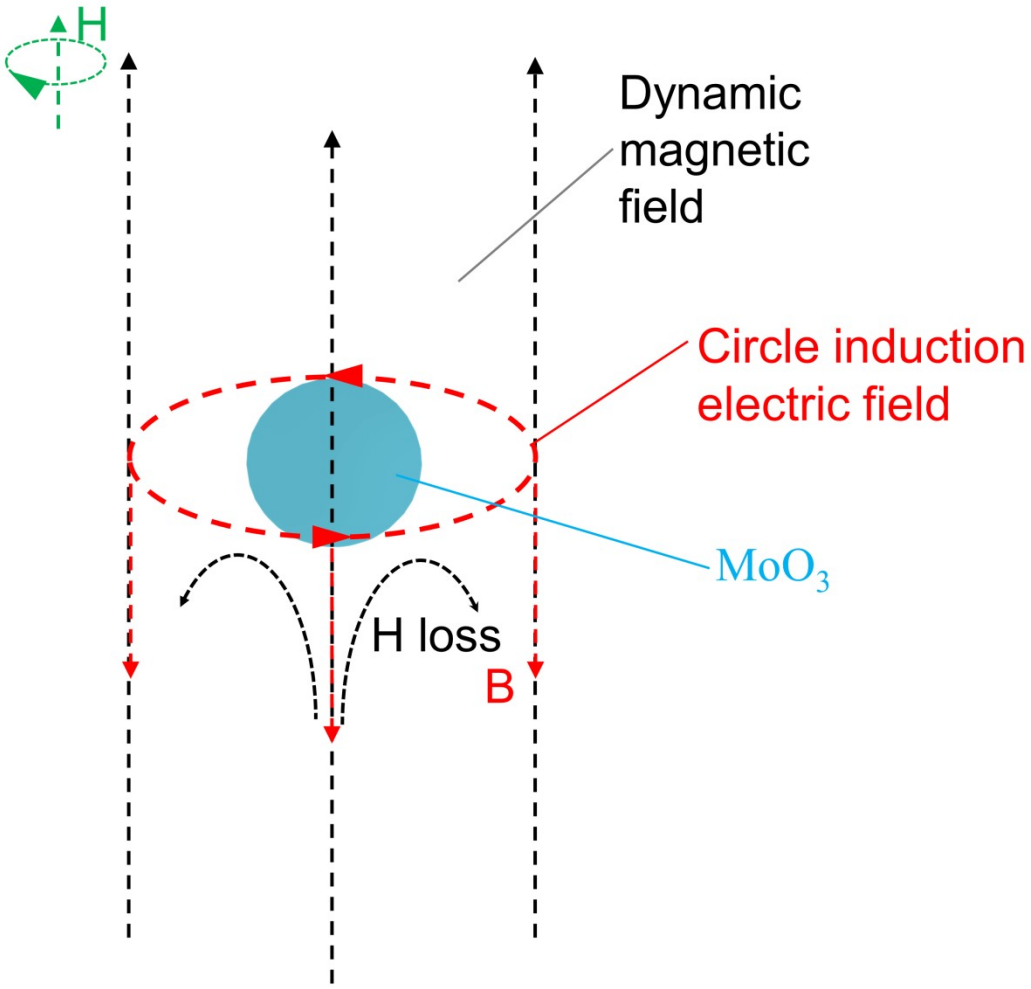

Fig. S2 Schematic representation of the interaction of a polar molecule of MoO_3 with a dynamic magnetic field.

3. **Based on the nucleation, MoS_2 nanosheets grow perpendicular to the substrate direction. The MoS_2 nanosheets grew and filled the substrate surface as the growth proceeded.**

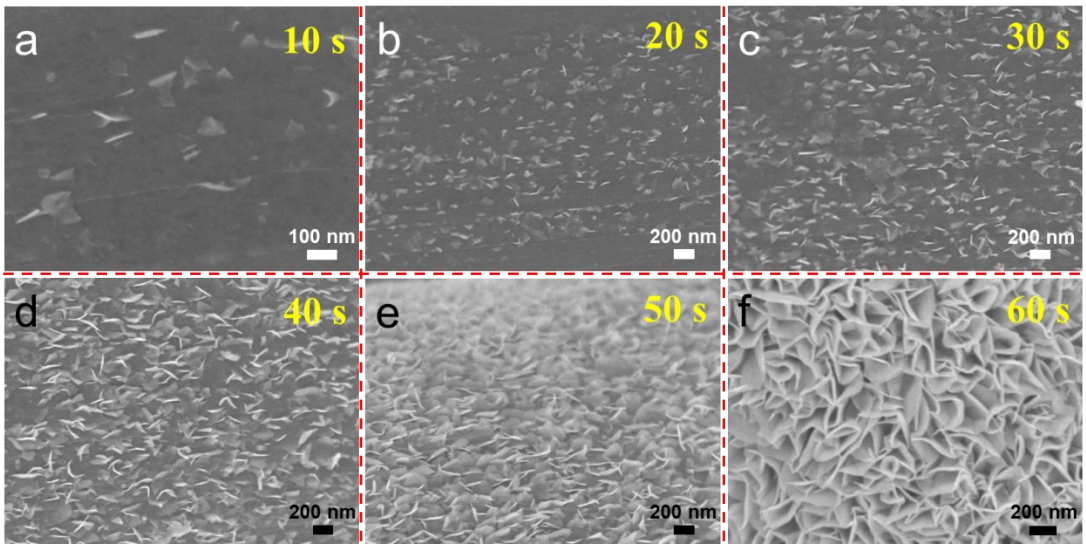

Fig. S3 The SEM images show the evolution of MoS_2 nanosheets on the surface of the grown carbon cloth over time, with a time interval of 10 seconds.

4. **The membrane composed of MoS_2/Mo-60 show a contact angle of 140°, which is close to superhydrophobicity。In addition, bubble contact experiments under water showed that SSF exhibited properties similar to 'Superaerophobic,' with a contact angle of 146°.**

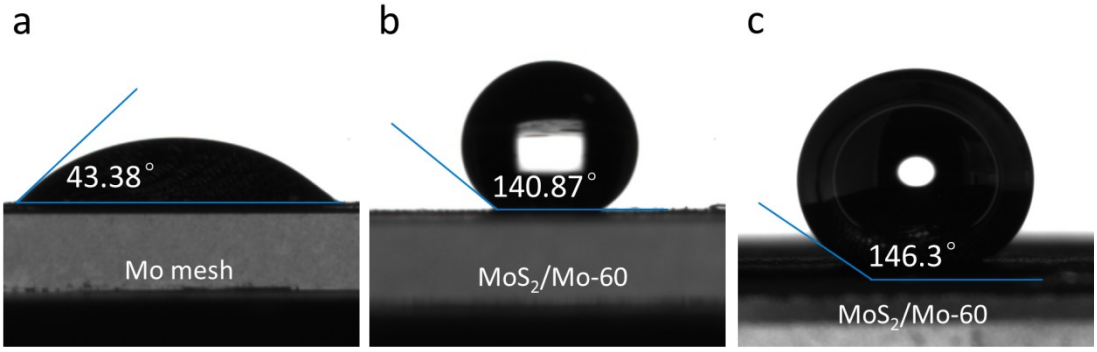

Fig. S4 Contact angle of Mo mesh and MoS_2/Mo-60.

5. **The original carbon fiber diameters were subjected to statistical analysis, revealing that most carbon fiber diameters cluster around 9.5um.**

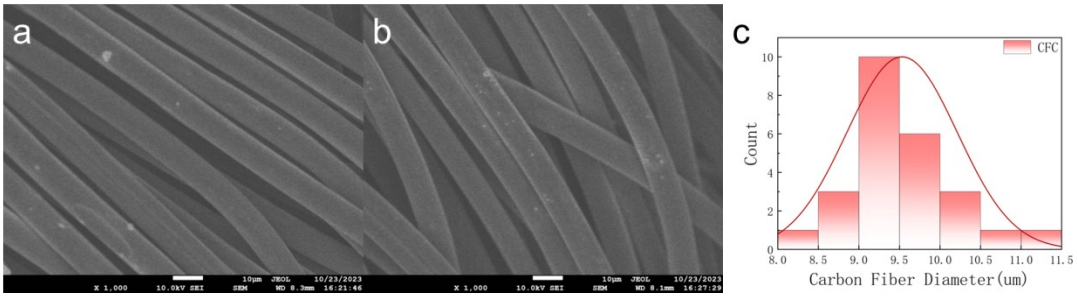

Fig. S5 (a) (b) shows the morphology of the original carbon fiber cloth. (c) show the statistics of carbon fiber diameters, with a median of around 9.5um.

6. The Raman spectra of MoS_2/C-60, MoS_2/Mo-60, MoS_2/W-60, and MoS_2/Ti-60 were obtained. There are two distinct characteristic Raman peaks within the range of Raman shifts from 350 to 450 cm^{-1}.

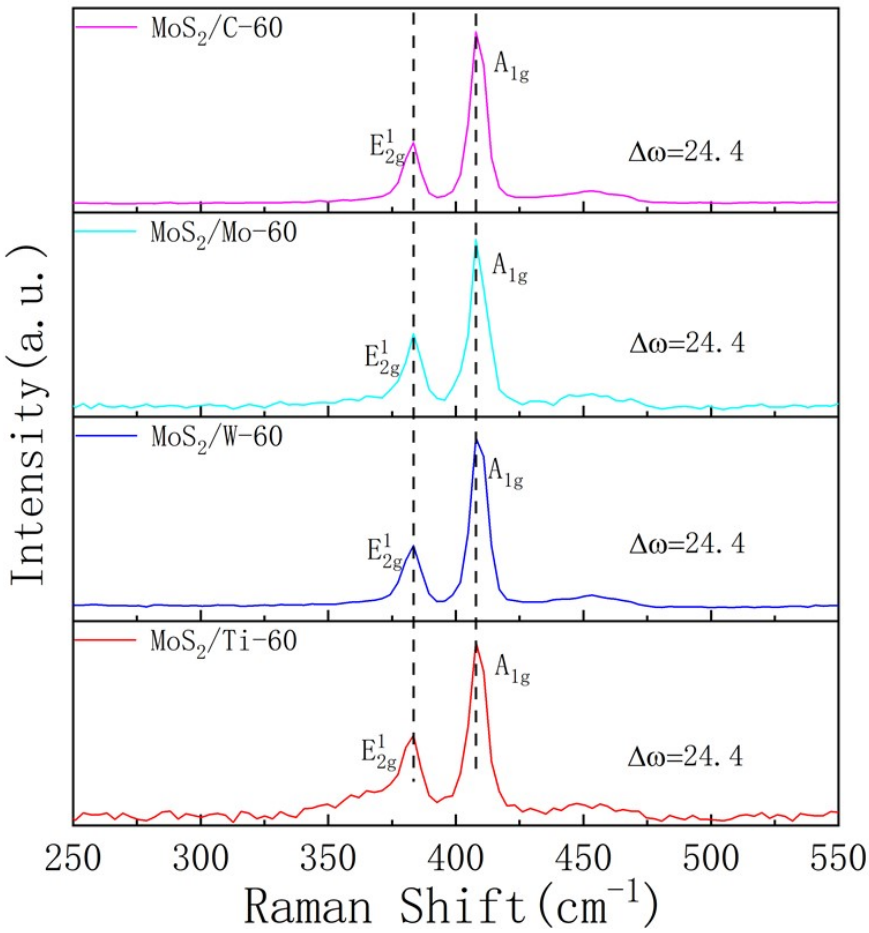

Fig. S6 The values of Δω for MoS_2/Mo-60, MoS_2/W-60, and MoS_2/Ti-60 are 24.4 cm^{-1}, which indicates that the thickness of MoS_2 nanosheets does not vary depending on the substrate.

7. The HETEM image of MoS_2 confirms the high quality of the crystalline structure.

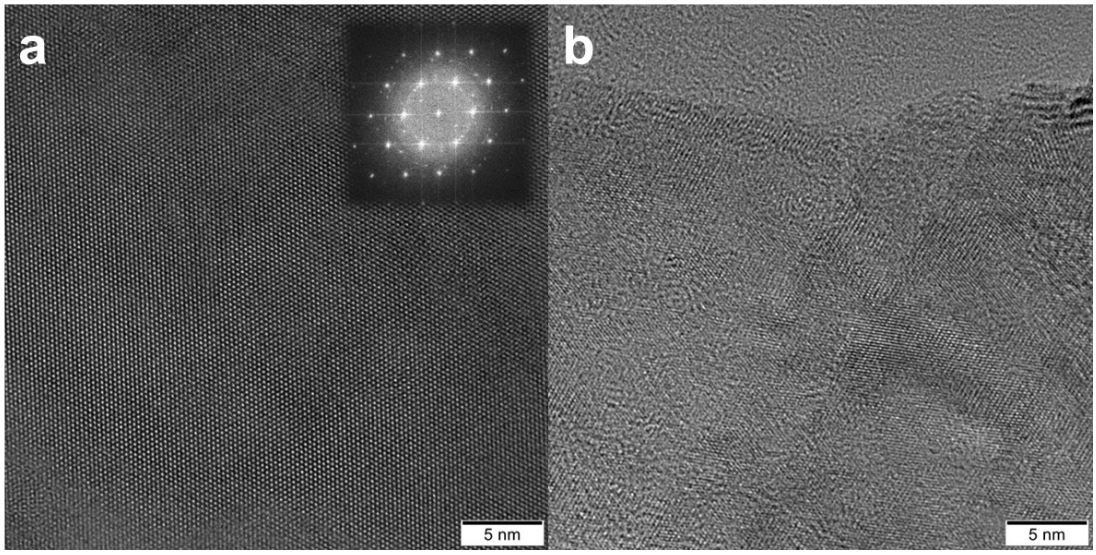

Fig. S7 (a) The HETEM image of MoS_2 confirms the high quality of the crystalline structure. (b) shows the triple stacking morphology of MoS_2/C-90 in the [010] direction.

8. A plot of thickness vs. deposition time data.

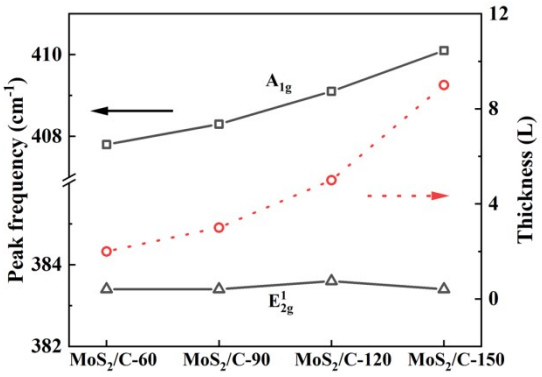

Fig. S8 Frequencies of E_{2g}^{1} and A_{1g} Raman modes (left vertical axis) and layer thickness seen in HRTEM (right vertical axis) as a function of deposition time.

9. Characterization of carbon cloth substrate, MoS_2/C-60, MoS_2/C-90, MoS_2/C-120, and MoS_2/C-150, from bottom to up in turn.

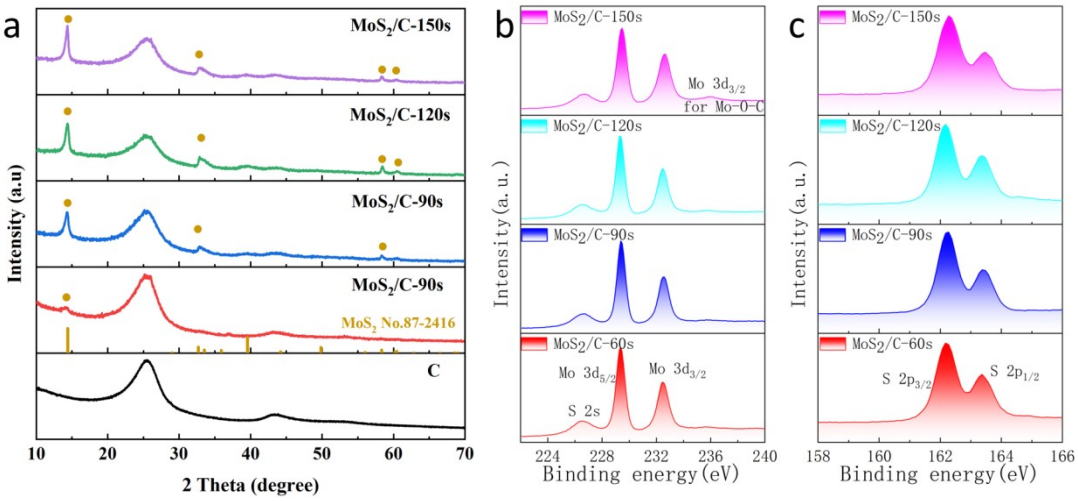

Fig. S9（Color in Online）Characterization of carbon cloth substrate, MoS_2/C-60, MoS_2/C-90, MoS_2/C-120, and MoS_2/C-150,from bottom to up in turn.(a) The XRD pattern of MoS_2, no impurity peaks of 2H-MoS_2 can be observed (standard PDF#87-2416). The peaks with marked orange circles represent the formed MoS_2. (b-c) XPS images of 2H-MoS_2 nanosheets at reaction times of 60 seconds (s), 90 s, 120 s, and 150 s. The presence of Mo-O-C bonds is evidenced by the broad peak observed at 235.8 eV.

10. The broad peak observed at 235.8 eV in the Mo 3d XPS spectrum can be attributed to the presence of a Mo-O-C bond, indicating the bonding between MoS_2 and carbon fibers.

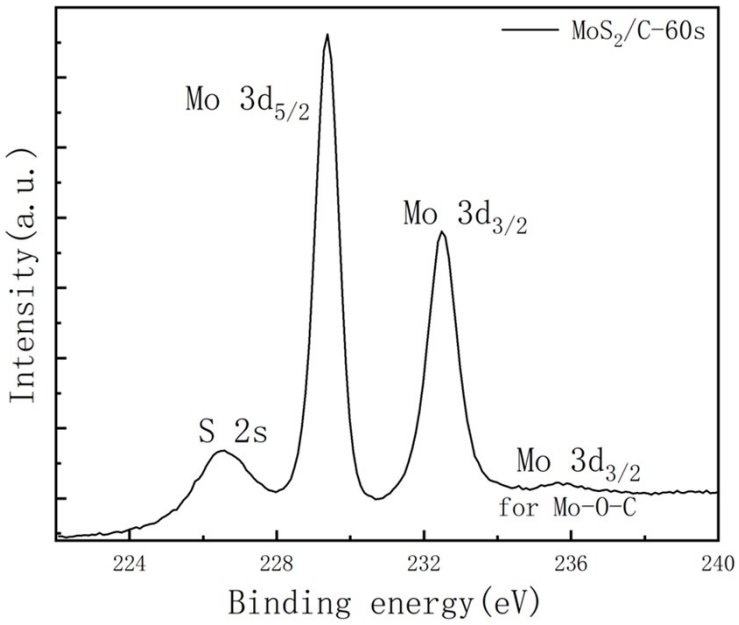

Fig. S10 The magnification of the Mo 3d energy level of MoS_2/C-60 reveals a broad peak at approximately 235.8 eV .

11. The SEM image shows the transition layer between MoS_2 and carbon cloth.

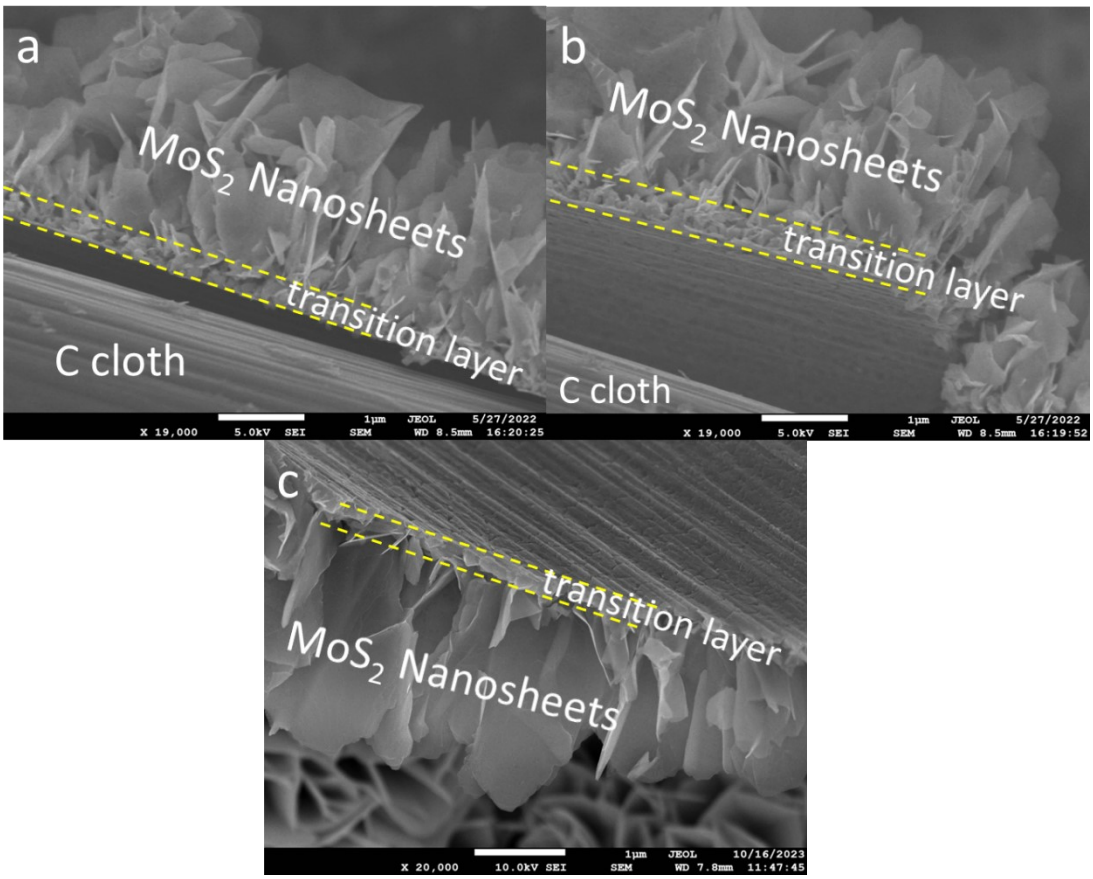

Fig. S11 The dense transition layer fixes the catalytic layer tightly to the substrate surface and covers even irregular surfaces.

12. The catalyst's effective electrochemically active surface area (ECSA) was estimated by electrochemical double-layer capacitance (C_{dl}).

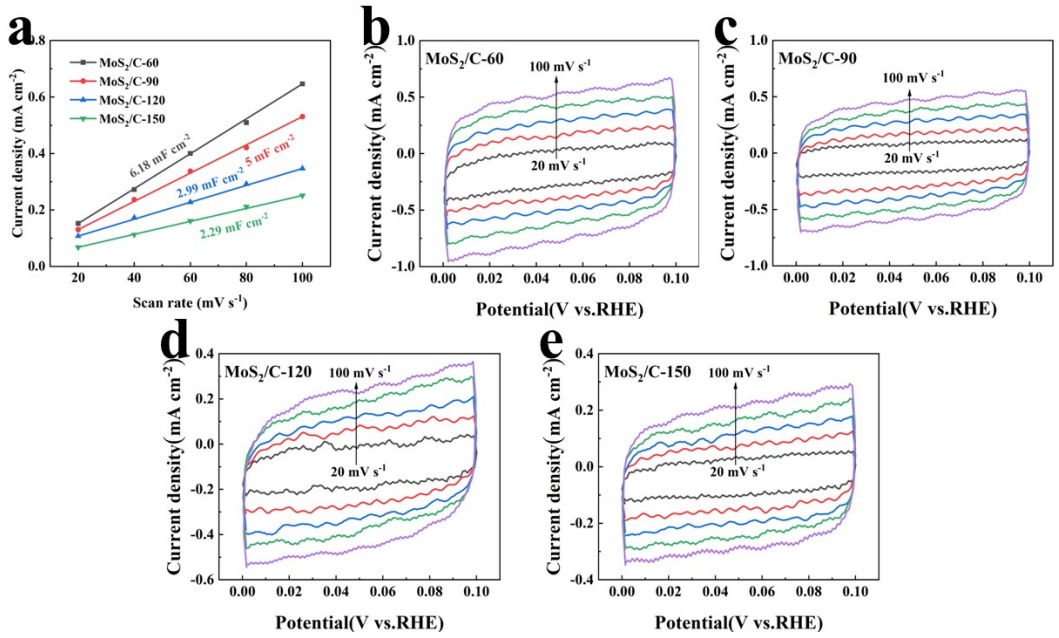

Fig. S12 C_{dl} extraction plots of MoS_2 nanosheets grown on carbon cloth at different reaction times. (b-d) CV curves of MoS_2/C-60、MoS_2/C-90、MoS_2/C-120 and MoS_2/C-150 in the region of 0.1-0.2 V (vs. RHE).

13. The catalyst's effective electrochemically active surface area (ECSA) was estimated by electrochemical double-layer capacitance (C_{dl}).

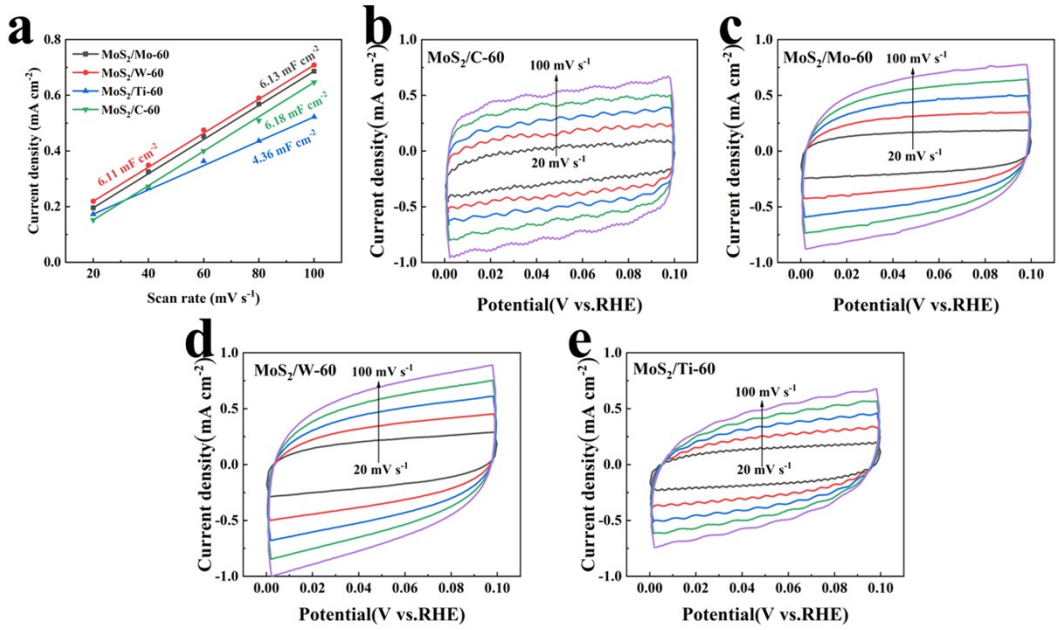

Fig. S13 C_{dl} extraction plots of MoS_2 nanosheets grown on different substrates. (b-d) CV curves of MoS_2/C-60、MoS_2/Mo-60、MoS_2/W-60 and MoS_2/Ti-60 in the region of 0.1-0.2 V (vs. RHE).

14. The MoS_2 nanosheets grown on the Mo mesh maintain their original structure after the catalyst electrode has been operated for a long time and impacted by many air bubbles.

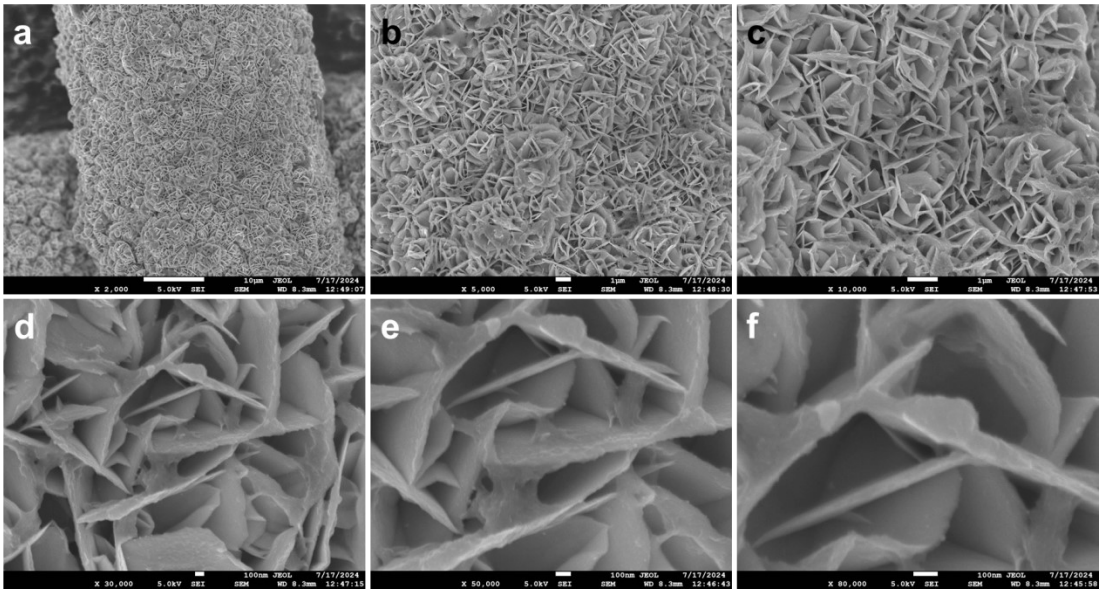

Fig. S14 SEM image of MoS_2/Mo-60 after 24 hours of CP testing.

15. Experimental

Growth of MoS_2 nanosheets

Molybdenum plates and various substrates (carbon cloth, molybdenum mesh, tungsten mesh, and titanium mesh) used in the experiments were ultrasonically cleaned with acetone, alcohol, and deionized water for 30 min each. The molybdenum plate, molybdenum trioxide, and sulfur are placed in the crucible. The substrate was trimmed into 10*13 mm rectangular electrodes and positioned vertically on the inner side of the crucible (Fig.1). The crucible was placed within a vacuum magnetic levitation induction furnace, with the induction coil current set to 50 A.The pressure within the chamber has been set at 5 kPa. The reactions were conducted at different reaction times. In the article, the samples of MoS_2 grown on carbon cloth with reaction times of 60s, 90s, 120s, and 150s were designated as MoS_2/C-60, MoS_2/C-90, MoS_2/C-120, and MoS_2/C-150, respectively. The MoS_2 samples grown on molybdenum，tungsten and titanium mesh with a reaction time of 60 s were named MoS_2/Mo-60, MoS_2/W-60 and MoS_2/Ti-60. Please refer to the supporting information for a more detailed description of the experimental methodology (Fig.S15).

The name of the equipment is called high-frequency induction heating furnace. Fig. S15 shows a sketch of the entire device. Fig. S15(b) shows a cross-sectional view of the corundum crucible. Copper coil damage caused by high temperatures is prevented by passing cooling water through the coil. When the power is turned on and current is applied to the coil, high frequency dynamic

magnetic field will be generated in the coil.

The dynamic magnetic field is coming from the field changing with time. Otherwise, we call it as static field. If we use “B” as the intensity of the magnetic field, the “B” changing with the time can be expressed as the function: B= $\frac{\mu_0 * N * I}{L}$, where the μ_0 is permeability of vacuum, and N represents turns per coil, and L is loop length，and I is electric current. The induction furnace equipment utilises an IGBT power supply. The function of this power supply is to rectify the negative signal of the current to the positive signal, thus maintaining the direction of the magnetic field. Consequently, the direction of the force remains unaltered throughout the experiment.So I=$I_m * |\sin(\omega t + \varphi)|$. Where the amplitude of the alternating current is represented by I_m, the angular frequency by ω, and the initial phase by φ. Since the ω= 2πf , f is frequency，therefore the B= $\frac{\mu_0 * N}{L} * I_m * |\sin(2\pi f t + \varphi)|$. Here, a current frequency of 50 kHz was adopted.

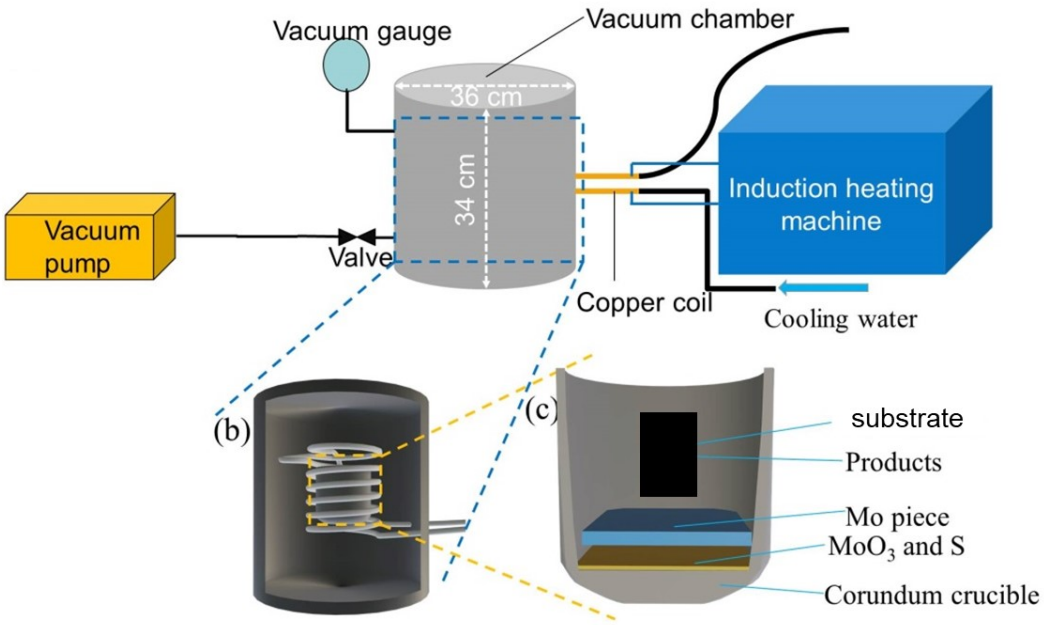

Fig. S15 Sketch of high-frequency induction-heated furnaces.

Characterizations

The crystalline phase of the resulting material was identified using an X-ray diffract meter (EMPYREAN). The material composition was determined using an X-ray photoelectron spectrometer (Thermo Scientific K-Alpha+). The morphology of the materials was observed by field emission transmission electron microscopy (FETEM) (JEM-F200, operating at 200 kV) and field emission scanning electron microscopy (FESEM) (JSM-7610F, operating at 5.0 kV). Raman spectra war obtained using a HORIBA XploRA PLUS Raman system under a 532 nm laser.

Electrochemical Measurements

Electrochemical catalytic were carried out in 0.5 M H_2SO_4 electrolyte degassed by Ar gas in a standard three-electrode system on a electrochemical workstation (CHI 760E chenghua, shanghai). In all measurements, an Ag/AgCl electrode

(saturated KCl electrolyte solution inside) was used as reference electrode，and graphite rod was used as the counter electrode. The MoS_2 nanosheets grown on a variety of substrates could be directly applied in the working electrode without any binder or conductive agent. The catalyst loading was determined by weighing the mass of the substrate before and after the reaction. In this work, all potentials mentioned were calibrated and related to the reversible hydrogen electrode (RHE) by the following equation: E(RHE) = E(Ag/AgCl) + 0.198 + 0.059×pH(V). Linear sweep voltammetry (LSV) curves were obtained with iR-compensation at a scan rate of 5 mV s^{-1}. The C_{dl} was calculated using CV curves at 0.1–0.2 V (vs RHE) at various scan rates. Electrochemical impedance spectroscopy (EIS) measurements were conducted at a potential of −0.25 V (vs. RHE) within the frequency range of 0.1 Hz to 100 kHz at an AC amplitude of 5 mV.